Structural basis for the Complement Alternative Pathway C3 convertase stabilization by Properdin

Martin Alcorlo[1], Agustín Tortajada[1,2], Santiago Rodríguez de Córdoba[1,2,$] and Oscar Llorca[1,$]

1) Centro de Investigaciones Biológicas, Consejo Superior de Investigaciones Científicas; and 2) Centro de Investigación Biomédica en Enfermedades Raras, Ramiro de Maeztu 9, 28040 Madrid, Spain

[$] Corresponding authors: Prof. Oscar Llorca

ollorca@cib.csic.es

+34 91 7373112 x4446 (tel)

+34 91 5360432 (fax)

Prof. Santiago Rodríguez de Córdoba

srdecordoba@cib.csic.es

+34 91 7373112 x4432 (tel)

+34 91 5360432 (fax)

Keywords: properdin, C3b, AP C3 convertase, complement, electron microscopy, EM

Running title: Structure of properdin-AP C3 convertase complex

Abstract

Complement is an essential component of innate immunity. Its activation results in the assembly of unstable protease complexes, denominated C3/C5-convertases, leading to inflammation and lysis. Regulatory proteins inactivate C3/C5-convertases on host surfaces to avoid collateral tissue damage. On pathogen surfaces, properdin stabilizes C3/C5-convertases to efficiently fight infection. How properdin performs this function is, however, unclear. Using electron microscopy we show that the N- and C-terminal ends of adjacent monomers in properdin oligomers conform a curly vertex that holds together the two components of C3-convertases, C3b and Bb. Properdin promotes a large displacement of the TED domain of C3b that impairs C3-convertase inactivation by regulatory proteins. The combined effect of molecular crosslinking and structural reorganization increases stability of the C3-convertase and facilitates recruitment of fluid-phase C3-convertase to the cell surfaces. Our model explains how properdin mediates the assembly of stabilised C3/C5-convertase clusters, which helps to localise complement amplification to pathogen surfaces.

\body

Introduction

Complement is a crucial component of the innate immunity. It is a first line defence mechanism against pathogens and it is essential in the modulation of the adaptive immune responses and to remove apoptotic cell debris and immune complexes (1). Activation of complement results in the formation of unstable protease complexes, named C3 convertases (C3bBb in the Alternative Pathway (AP)), which catalyse the cleavage of C3 to generate the activated fragment, C3b. This exposes a reactive thioester that attaches covalently to the target surfaces (opsonization), initiating the terminal pathway that causes cell lysis and generates inflammation at the site of activation (1, 2).

The complement AP is exquisitely regulated, as both undesired defective or excessive activity associates with pathological conditions (2). Accelerated dissociation of the AP C3 convertase and inactivation of C3b are critical steps to maintain complement homeostasis and to prevent non-specific damage to self-cellular components when complement is activated. These activities are performed primarily by factor H (FH), in collaboration with the plasma serine protease factor I (FI) (2). Self-tissues are also protected by membrane-bound proteins that restrict complement activation by acting as cofactor for proteolytic inactivation of C3b by FI or accelerating the dissociation of the C3bBb convertase. Thus, in health, spontaneous activation of C3 in plasma is kept at a low level and further complement activation and C3b deposition is restricted to targets lacking surface regulators. Recent advances in understanding the structural basis of the assembly, activation and regulation of the AP C3 convertase have provided important insights into the regulation of the AP and the pathogenic consequences of its dysregulation (2-4).

Properdin is the only known complement regulator that enhances the stability of the C3bBb convertase and the activity of the AP. Properdin binds to C3bB and C3bBb more efficiently than to C3b alone, stabilising pre-formed C3bBb convertase complexes (5). Properdin is also a pattern-recognition molecule that binds to negatively charged molecules on certain microbial surfaces, apoptotic and necrotic cells, as well as cells undergoing malignant transformation. Once bound to a surface, properdin can direct C3b deposition and C3bBb assembly, thus serving as a focal point for amplifying complement activation (6). Although the importance of properdin has been somehow neglected, it plays important roles in antibacterial defence and in inflammatory or autoimmune diseases, as illustrated by the high vulnerability of properdin-deficient individuals to *Neisseria meningitides* infections and the reported role of properdin in a number of pathological conditions (7, 8).

Properdin is a 53-kDa glycoprotein comprising seven conserved domains with homology to thrombospondin repeats (TSRs) of type I, and numbered TSR0 to TSR6 from the N- to the C- terminus (**Fig. 1A**) (9). Atomic structures for properdin have not been resolved yet, but the structure of a double-TSR domain from thrombospondin (PDB 3R6B) provides a reasonable model for TSR domains in properdin (10) (**Fig. 1A**). Each TSR comprises a folded core consisting of three antiparallel strands (A, B and C) held together by three disulfides (11) (**Fig. 1A**). Human plasma contains a low concentration of properdin (0.02 mg/ml) in the form of a polydisperse mixture of oligomeric structures, mostly dimers, trimers and tetramers (12). Examination of purified properdin using electron microscopy (EM) revealed that each monomer forms an elongated rod-like molecule, which associates into cyclic polymers (13). How properdin stabilises C3bBb convertases is still unknown, which we reveal here by solving the architecture of the properdin-C3bBb complex.

Results

Intricate connections between properdin monomers assemble large oligomers

Human properdin was purified to homogeneity from plasma by immunoaffinity followed by ionic exchange and size exclusion chromatography (**Fig. 1B**). The functional integrity of the purified properdin was verified using AP-dependent hemolytic assays with rabbit erythrocytes (**Fig. S1**). Properdin was observed in the electron microscope and found assembled into several oligomeric species in which the elongated monomers were connected at their ends. As previously reported (12, 13) the most common oligomers were triangle-shaped trimers, squared-shaped tetramers and pentagonal pentamers (**Fig. 1C,** and below). From these EM images we interpreted that the interaction between properdin monomers involves the N-terminal end of one monomer and the C-terminal end of another, permitting the assembly of a variety of oligomers with the only restriction of geometrical constraints. Interestingly, we found that the angle formed by two adjacent monomers ranged from 60º in the trimers to 108º in the pentamers, indicating a large flexibility in the interaction between monomers.

Analysis of the vertex of the properdin oligomers by single-particle image processing methods revealed a complex structure. 6425 images of vertexes from the tetramers were extracted from the micrographs to be sorted into homogenous groups and averaged to improve the signal/noise ratio (**Fig. 1D**). The 3D structure of the vertex at 23.4 Å resolution revealed a connectivity between monomers that was very different to that proposed from X-ray scattering data and modelling (14) (**Fig. 1E**, **Fig. S1**). We modelled the number of TSR domains comprised by this vertex by manually fitting the atomic structure of one of the homologous TSR domain from thrombospondin (PDB ID 3R6B) (10) into the EM density. Each properdin monomer comprises seven TSR domains and we found that four of these units could be accommodated into the vertex. Thus, each properdin monomer contributes four TSR domains for the assembly of two vertexes, at the N- and C-terminal end of each monomer, leaving three TSR units for the elongated connection between vertexes. In agreement with

this, we found that the average distance between vertexes, obtained from 150 images of complexes, measured 14.3±1.2 nm (**Fig. 1F**), which fits the length spanned by three TSRs, assuming an averaged length of 5 nm per TSR domain based on the atomic structure (10).

Purification of the properdin-C3bBb convertase complex

We assembled the complex between properdin and C3 convertase by incubating C3b, FB and FD in the presence of properdin. In these experiments we used the FB-D279G mutant that increases the stability of C3 convertase (2). The mixture was resolved by gel filtration chromatography and the mobility of the complex compared to that of properdin alone. We observed co-migration of C3b, the Bb fragment of FB and properdin in a large molecular weight species compared to the elution of C3bBb convertase alone, indicating the formation of a complex containing C3bBb and properdin (**Fig. 2A**). The peak fraction was observed in the electron microscope, revealing properdin oligomers decorated by extra densities corresponding to C3bBb convertases (**Fig. 2B**). Interestingly, C3bBb convertase molecules were bound to properdin vertexes, revealing that the structure assembled by the oligomerization of two properdin monomers was essential for C3bBb convertase recognition. C3bBb molecules protruded outwards from these vertexes. We tested several concentrations of C3bBb convertase and found that the level of vertex occupancy was dependent on the amount of C3bBb convertase used in the experiment (**Fig. 2B**). This indicates that each properdin oligomer has the potential to use all its vertexes to bind C3bBb convertase (**Fig. 2C**).

Properdin crosslinks C3b and the Bb fragment, stabilizing the C3bBb convertase

The bases for C3bBb convertase stabilization by properdin were explored by processing 21891 images of C3bBb convertase molecules at properdin vertexes extracted from the micrographs. These images were computationally classified to find and average those corresponding to similar views of the complex (**Fig. 3A**). These averages were extremely revealing when compared to the crystal and EM structure of C3bBb convertase (15, 16). The MG ring and C345C domain from C3b, and the vWA and SP domains from FB were clearly identified, as well as the properdin vertex contacting C345C and vWA (**Fig. 3B**). Other averages were interpreted as corresponding to additional views of the complex from a different angle and these were used for the 3D analysis of the complex (see below). Surprisingly, the most typical view of the properdin-C3bBb convertase complex was found in two distinct sub-types, either containing or not a strong globular density in the proximity of MG3 domain (see below).

Images of the properdin-C3bBb convertase complex were then used to reconstruct its 3D structure. We found that two conformations were coexisting in the dataset, which corresponded with those images that either contained or not a globular density in the proximity of the MG3 domain. The data set was consequently split in two sub-groups (**SI Material and Methods**). The 3D structure of the major population solved at 29.3 Å resolution, corresponding to 66.6 % of the particles, was interpreted by fitting the atomic structure of C3bBb convertase (PDB ID 2WIN) (15) into the EM map to generate a hybrid pseudo-atomic model of the complex (**Fig. 3C**). The Bb fragment together with the C345C domain had to be moved backwards by ~30º in order to fit into the density of the EM map, indicating a displacement compared to the crystal structure. This is conceivable by the flexible linker connecting C345C to the MG ring, as observed in the EM images of C3bBb convertase (15, 16). The fitting revealed that a small segment of the MG ring corresponding to MG4 was not well resolved in the reconstruction, which we interpret as an effect of the

accumulation of staining agent in the centre of the MG ring by the proximity of the globular density in MG3. Remarkably, we found that the TED domain was missing at its expected location in C3b, strongly suggesting that the globular density in the vicinity of the MG ring corresponds to the TED domain.

The structure revealed that properdin contacts both, the C345C domain in C3b and the vWa domain in Bb (**Fig. 3C**), indicating that properdin stabilizes the C3bBb convertase by holding together the two components of this enzymatic complex. The structure also suggested that properdin would interact with these two domains more efficiently when the Bb fragment is in the conformation found in C3bBb convertase than the closed conformation of the C3bB proconvertase. We confirmed this hypothesis after observing that properdin did not interact with the complex between C3b homolog Cobra Venom factor (CVF) and FB, since CVF and FB form a tight complex but FB is maintained in its closed conformation (17) (**Fig. 3D**).

Properdin promotes a relocation of the TED domain

The 3D structure of the minor population of properdin-C3bBb convertase complexes revealed essentially the same structural features of the most abundant conformation albeit at lower resolution, but the TED domain was at its expected location in C3b (**Fig. S2A-S2B**). Thus, the TED domain was found in two positions in the context of the properdin-C3bBb convertase complex, at approximate 1:2 ratio between the two species (33.3% *vs* 66.6%). We searched for this conformation of the TED domain in the C3b preparation used for these studies by collecting single molecule images, which were classified and averaged as before (**Fig. S2C**). We found that only 3.5 % of 5000 images of C3b showed this unusual conformation, whereas ~73 % corresponded to the TED position described in the crystal structure (2-4). Interestingly,

~18 % of the images revealed alternative locations for the TED domain. As a whole, these results indicate that properdin stimulates the rearrangement of the TED domain in C3b.

Properdin interferes with C3bBb convertase decay

The repositioning of the TED domain is predicted to remove essential structural determinants for the interaction of C3b with the complement regulators FH, DAF and CR1, turning the properdin-C3bBb complex less prone to accelerated decay compared to C3bBb alone (4, 18). Similarly, the repositioning of the TED domain should impair the interaction between C3b and Membrane cofactor protein (MCP or CD46) slowing down the FI-dependent proteolytic inactivation of C3b. We tested this hypothesis by assembling a C3bBb convertase through the incubation of C3b, FB and FD in the absence or presence of properdin (**Fig. S2D**). Next, MCP and FI were added and incubated for 15 min in all cases, to allow for cofactor activity. We observed that the amount of intact C3b remaining after the incubation, quantified as the ratio between α´chain/β chain of C3b (**Fig. S2E**), was significantly reduced in the presence of properdin in a dose-dependent manner. These data show that properdin stabilize the C3bBb convertase by reduceing the accelerated decay by the complement regulators.

Structural model for properdin-C3bBb complexes

We combined the information provided by the EM images to model the structure of the oligomeric properdin-C3bBb convertase (**Fig. 4A**). Each properdin vertex has the potential to bind and stabilise one molecule of the C3bBb complex. The structure of each of these vertexes could be interpreted as combinations of 2-2, 1-3 or 0-4 TSR units from each of the two contacting monomers and we could not discriminate between these options at the resolution of these studies. Experiments using recombinant forms of properdin, where some

TSR domains were truncated, showed that TSR3, TSR4 and TSR5 were not essential for oligomerization, whereas TSR6 was strictly required (19). TSR0, TSR1 and TSR2 were not included in those studies. Since we found four TSR domains involved in oligomerization, this suggests a model where TSR0, TSR1 and TSR2 from one monomer and TSR6 from another monomer interact to form the vertex (**Fig. 4B**). TSR4 and TSR5 mutants showed some defects in oligomerization as they could assemble as dimers, but not higher order oligomers (19), and therefore, other models involving TSR4 and TSR5 in vertex formation are conceivable (**Fig. 4B**).

Discussion

A major point of regulation in the activation of complement is altering the stability of the alternative pathway C3bBb convertase. Down-regulation to control homeostasis and prevent tissue damage is provided by a number of plasma and membrane-associated regulators that accelerate the dissociation of the C3bBb complex (3). In contrast, properdin is the only complement regulator that stabilizes the C3bBb convertase, which may be critical to tip the balance in favour of amplification on microbial pathogens (9). The molecular bases of the properdin functions are still poorly understood. Using EM single-particle image processing methods we describe here a structural model for the properdin- C3bBb complex supporting that properdin stabilizes the C3bBb convertase by holding together the two components of the AP C3 convertase, C3b and Bb, and by promoting a large displacement of the TED domain that likely interferes with the decay of C3 convertase by complement down-regulators.

Properdin oligomerizes by a complex interplay between N- and C-terminal ends of two elongated monomers forming a curly vertex structure. This interaction allows the assembly of oligomers containing a variable number of monomers, and the maximum number

of units that could be accommodated per oligomer is probably only limited by conformational and geometrical restrains. Each vertex is the structural unit of recognition and stabilization of C3bBb convertase by holding together the C345C and the vWA domains from C3b and Bb, respectively. Thus, oligomerization, which requires the involvement of the N- and the C-terminal TSRs, is essential for recognition of C3bBb convertase. The studies by Higgins et al. (1995), which proposed functions for several TSR domains in properdin by characterising recombinant properdin lacking single specific TSRs (19), need to be re-interpreted, as any mutation affecting oligomerization would indirectly affect C3bBb binding. The involvement of TSR6 at the vertex in stabilization of C3bBb is supported by the disease-associated Y387D mutation in TSR6 that produces normal plasma levels of properdin that assembles oligomer lacking the capability to stabilise the C3bBb convertase (20).

A remarkable finding is the positioning of the TED domain in two alternative locations, one in agreement with the crystal structure of C3b and an alternative location in the vicinity of the MG3 domain. Such movement appears to be an intrinsic property of C3b, as we find a similar conformation in a small percentage of C3b molecules, but certainly properdin turns this alternative conformation into the major species. In agreement with our findings, previous EM studies by Nishida N. *et al*. found a proportion of C3b molecules in this alternative conformation (21). In addition, recent FRET data obtained for C3b in complex with SCR1-4 from FH suggested some degree of mobility of the TED domain (22). Large displacements of the CUB-TED region seem feasible as these take place during the structural transition from C3 to C3b (4) and also from C3b to iC3b (23).

The rearrangement of the TED domain removes essential structural determinants for recognition of C3b by some regulators such as FH and MCP (4). SCR1-4 of FH interacts with C3b as an elongated string of monomers and this causes decay of C3 convertase, as revealed in the crystal structure of this complex (18). Movements of the TED domain in iC3b, a

proteolytic fragment of C3b, have been shown to disrupt FH binding and consequentially iC3b is not regulated by FH (23). Similarly, the rearrangements of the TED domain that we find in the properdin-C3bBb convertase complex would limit C3 convertase regulation by FH, MCP and other regulators that use similar mechanisms, such as DAF. In agreement with this interpretation, we observed a reduced FI-dependent cofactor activity of MCP for the proteolysis of C3b in the presence of properdin. We speculate this will contribute, in addition to the holding of C3b and Bb together, to enhance the complement responses *in vivo*.

Materials and Methods

Generation and purification of properdin-C3bBb convertase complexes. C3b and properdin were purified from plasma y FB from the supernatant of CHO cells. C3b (5 μg), FB (10 μg, FB or FB-D279G) and properdin (P, 1 μg) were incubated for 35 min at room temperature in 20 mM Hepes (pH 7.5), 75 mM NaCl and 5 mM $MgCl_2$ at a final molar ratio P:C3b:FB 0.7:1:4. Subsequently, 100 ng of FD (Calbiochem) were added and the mixture was injected in a Superdex 200 column (GE Healthcare). Fractions were analysed using 10% SDS/PAGE.

Electron Microscopy and Image processing. A few microliters of freshly purified were adsorbed onto carbon-coated grids and negatively stained with 2% (mass/vol) uranyl formate. Micrographs were recorded using a JEOL 1230 transmission electron microscope and a 4 k x 4 k TVIPS detector using EM-TOOLS (TVIPS). Images were collected at a final magnification of 54926x. 6425 images for properdin vertexes and 19805 images for C3bBb convertases bound to a propedin vertex were selected and processed using EMAN (24). *Ab initio* templates for refinement were obtained using the command *e2initial model* in EMAN2 (24) and the random conical tilt (RCT) method.

See also **SI Materials and Methods**.

ACCESSION NUMBERS

The 3D-EM maps of the properdin vertex and properdin-C3bBb convertase have been deposited in the 3D EM database (http://www.ebi.ac.uk/msd/) under accession codes ***** and *****, respectively (to be provided upon acceptance).

ACKNOWLEDGEMENTS

This work was funded by the Autonomous Region of Madrid (S2010/BMD-2316 to SRdC and OL), the "Ramón Areces" Foundation (to OL), and the Spanish Government (SAF2011-22988 to O.L., SAF2011-26583 to SRdC); Martin Alcorlo is a Sara Borrell fellow from the "Instituto de Salud Carlos III" (CD09/00282). OL is additionally supported by "Red Temática de Investigación Cooperativa en Cáncer (RTICC)" (RD06/0020/1001). SRdeC is also supported by the Fundación Renal Iñigo Alvarez de Toledo and the 7FP European Union project EURenOmics. We thank our colleagues at the lab of Santiago Rodriguez de Cordoba for their help in the purification of C3b, FB and properdin.

References

1. Ricklin D, Hajishengallis G, Yang K, & Lambris JD (2010) Complement: a key system for immune surveillance and homeostasis. (Translated from eng) *Nat Immunol* 11(9):785-797 (in eng).
2. Rodriguez de Cordoba S, Harris CL, Morgan BP, & Llorca O (2011) Lessons from functional and structural analyses of disease-associated genetic variants in the complement alternative pathway. (Translated from eng) *Biochim Biophys Acta* 1812(1):12-22 (in eng).
3. Gros P, Milder FJ, & Janssen BJ (2008) Complement driven by conformational changes. (Translated from eng) *Nat Rev Immunol* 8(1):48-58 (in eng).
4. Lea SM & Johnson S (2012) Putting the structure into complement. (Translated from eng) *Immunobiology* 217(11):1117-1121 (in eng).
5. Hourcade DE (2006) The role of properdin in the assembly of the alternative pathway C3 convertases of complement. (Translated from eng) *J Biol Chem* 281(4):2128-2132 (in eng).
6. Spitzer D, Mitchell LM, Atkinson JP, & Hourcade DE (2007) Properdin can initiate complement activation by binding specific target surfaces and providing a platform for

de novo convertase assembly. (Translated from eng) *J Immunol* 179(4):2600-2608 (in eng).

7. Densen P (1989) Interaction of complement with Neisseria meningitidis and Neisseria gonorrhoeae. (Translated from eng) *Clin Microbiol Rev* 2 Suppl:S11-17 (in eng).
8. Lesher AM*, et al.* (2013) Combination of factor H mutation and properdin deficiency causes severe C3 glomerulonephritis. (Translated from eng) *J Am Soc Nephrol* 24(1):53-65 (in eng).
9. Kemper C, Atkinson JP, & Hourcade DE (2010) Properdin: emerging roles of a pattern-recognition molecule. (Translated from eng) *Annu Rev Immunol* 28:131-155 (in eng).
10. Klenotic PA, Page RC, Misra S, & Silverstein RL (2011) Expression, purification and structural characterization of functionally replete thrombospondin-1 type 1 repeats in a bacterial expression system. (Translated from eng) *Protein Expr Purif* 80(2):253-259 (in eng).
11. Chondrou M, Papanastasiou AD, Spyroulias GA, & Zarkadis IK (2008) Three isoforms of complement properdin factor P in trout: cloning, expression, gene organization and constrained modeling. (Translated from eng) *Dev Comp Immunol* 32(12):1454-1466 (in eng).
12. Pangburn MK (1989) Analysis of the natural polymeric forms of human properdin and their functions in complement activation. (Translated from eng) *J Immunol* 142(1):202-207 (in eng).
13. Smith CA, Pangburn MK, Vogel CW, & Muller-Eberhard HJ (1984) Molecular architecture of human properdin, a positive regulator of the alternative pathway of complement. (Translated from eng) *J Biol Chem* 259(7):4582-4588 (in eng).
14. Sun Z, Reid KB, & Perkins SJ (2004) The dimeric and trimeric solution structures of the multidomain complement protein properdin by X-ray scattering, analytical ultracentrifugation and constrained modelling. (Translated from eng) *J Mol Biol* 343(5):1327-1343 (in eng).
15. Rooijakkers SH*, et al.* (2009) Structural and functional implications of the alternative complement pathway C3 convertase stabilized by a staphylococcal inhibitor. (Translated from eng) *Nat Immunol* 10(7):721-727 (in eng).
16. Torreira E, Tortajada A, Montes T, Rodriguez de Cordoba S, & Llorca O (2009) 3D structure of the C3bB complex provides insights into the activation and regulation of

the complement alternative pathway convertase. (Translated from eng) *Proc Natl Acad Sci U S A* 106(3):882-887 (in eng).

17. Janssen BJ*, et al.* (2009) Insights into complement convertase formation based on the structure of the factor B-cobra venom factor complex. (Translated from eng) *EMBO J* 28(16):2469-2478 (in eng).
18. Wu J*, et al.* (2009) Structure of complement fragment C3b-factor H and implications for host protection by complement regulators. (Translated from eng) *Nat Immunol* 10(7):728-733 (in eng).
19. Higgins JM, Wiedemann H, Timpl R, & Reid KB (1995) Characterization of mutant forms of recombinant human properdin lacking single thrombospondin type I repeats. Identification of modules important for function. (Translated from eng) *J Immunol* 155(12):5777-5785 (in eng).
20. Fredrikson GN*, et al.* (1996) Molecular characterization of properdin deficiency type III: dysfunction produced by a single point mutation in exon 9 of the structural gene causing a tyrosine to aspartic acid interchange. (Translated from eng) *J Immunol* 157(8):3666-3671 (in eng).
21. Nishida N, Walz T, & Springer TA (2006) Structural transitions of complement component C3 and its activation products. (Translated from eng) *Proc Natl Acad Sci U S A* 103(52):19737-19742 (in eng).
22. Pechtl IC, Neely RK, Dryden DT, Jones AC, & Barlow PN (2011) Use of time-resolved FRET to validate crystal structure of complement regulatory complex between C3b and factor H (N terminus). (Translated from eng) *Protein Sci* 20(12):2102-2112 (in eng).
23. Alcorlo M*, et al.* (2011) Unique structure of iC3b resolved at a resolution of 24 A by 3D-electron microscopy. (Translated from eng) *Proc Natl Acad Sci U S A* 108(32):13236-13240 (in eng).
24. Tang G*, et al.* (2007) EMAN2: an extensible image processing suite for electron microscopy. (Translated from eng) *J Struct Biol* 157(1):38-46 (in eng).

Figure Legends

Fig. 1. **Structure of properdin oligomers by electron microscopy**

(A) Schematic cartoon of the arrangement of TSR domains in a properdin monomer (upper panel) and a view of the atomic structure of one homologue TSR domain from thrombospondin (PDB ID 3R6B, lower panel) (10). Side chains of the proposed key arginine and tryptophan residues are shown in blue and yellow, respectively. Disulfide bonds are shown in pink.

(B) Final preparation of purified properdin analyzed by SDS-PAGE. SS: silver staining, CS: Coomassie staining, WB: western blotting using polyclonal antibodies against properdin.

(C) A typical micrograph of properdin. Selected single molecule images for several properdin oligomers are highlighted within a red square. Scale bar represents 26 nm.

(D) Reference-free 2D averages of properdin vertexes extracted from the micrographs reveal several views of the structure connecting two monomers. Scale bar corresponds to 7 nm.

(E) 3D structure of the properdin vertex and pseudo-atomic model obtained by fitting a crystal structure of a TSR domain from thrombospondin (PDB ID 3R6B) (10) into the EM density. Scale bar corresponds to 1.2 nm.

(F) Carton representation of a properdin tetramer (lower panel) and a raw image for a properdin tetramer (upper panel). Vertexes are represented as a blue circle and the region whose distance was measured is indicated.

Fig. 2. **Purification and electron microscopy of the properdin-C3bBb convertase complex**

(A) Chromatograms (upper panel) and silver-stained SDS-PAGE (lower panels) for the fractions of size-exclusion chromatography experiments performed in a Superdex 200 gel-filtration column (GE Healthcare) using properdin, C3b, FD and either wild type FB or the FB-D279G mutant. Chromatograms show profiles for properdin injected alone (P, blue line), the incubation of C3b, FB and FD to assemble a C3bBb convertase (C3bBb, magenta discontinuous line), and the incubation of properdin, C3b, FB-D279G and FD to assemble a properdin-C3bBb convertase complex (PC3bBb, green line). Bottom panels show SDS-PAGE of selected fractions from the chromatographies above. Left panels correspond to the assembly of a C3bBb convertase (C3bBb, magenta discontinuous line), whereas right panels correspond to the properdin-C3bBb convertase complex (PC3bBb, green line). Central panels show the SDS-PAGE of a chromatography (not shown) analysing the interaction of properdin with the C3bB proconvertase. In all experiments the input to the gel-filtration column is indicated as “IN”, and C3b, FB and properdin are loaded as controls. Chains of C3b detected in the SDS-PAGE are indicated. The formation of the properdin-C3bBb convertase complex is revealed by the advanced elution of C3bBb (factions 10-15) in the presence of properdin compared to the elution of C3bBb convertase alone (C3bBb, fractions 17-21), as well as the appearance of a new band corresponding to the FB fragment Bb (labelled “Bb”) resulting from the proteolysis of the input FB (labelled FB). The fraction selected for EM analysis is labelled.

(B) Representative micrograph corresponding to properdin-C3bBb convertase complexes collected at two experimental conditions generating partial (left panel) or high occupancy (right panel) of properdin by C3bBb convertase. Selected C3bBb convertase molecules bound to properdin have been labelled with an open arrow. Black arrows stand for unbound C3bBb convertase molecules. Scale bar corresponds to 14 nm.

(C) Gallery of raw images of properdin-C3bBb convertase complexes selected from the micrographs and panelled according to the oligomeric state of properdin, and showing, from left to right, increased occupancy of properdin vertexes with C3bBb convertase molecules. Scale bar corresponds to 14 nm.

Fig. 3. **Structure of the properdin-C3bBb convertase complex**

(A) Representative reference free 2D averages of C3bBb convertase molecules bound to properdin vertexes (right panels), compared to a view of the crystallographic and EM structures of C3bBb convertase (left panels) (PDB ID 2WIN) (15). Each domain has been coloured differently and labelled. Scale bar corresponds to 5 nm.

(B) Selected average of the properdin-C3bBb convertase complex. Different domains and regions are labelled. Scale bar corresponds to 5 nm.

(C) Two views of the structure of the properdin-C3 convertase complex at 29.3 Å resolution. A pseudo-atomic model of the properdin-C3 convertase complex was obtained by fitting the atomic structure of C3bBb convertase (PDB ID 2WIN) (15) into the EM structure. The MG ring is displayed in blue colour. C345, CUB and TED domains are coloured in orange, red and green respectively. vWA and SP domains from the Bb fragment are coloured in pink. Densities corresponding to properdin vertex are labelled with asterisks. Scale bar corresponds to 2 nm.

(D) Fractions from a size-exclusion chromatography loaded with the incubation of CVF, FB-D279 mutant, properdin and FD were analysed by SDS-PAGE. Properdin does not interact with CVF-FB in the conditions tested, as revealed by the absence of co-migration of the CVFB complex with properdin. Inset at the top right hand corner shows an average of images

obtained for the purified CVFB complex using electron microscopy. Scale bar corresponds to 5 nm.

Fig. 4. **Model for complement activation by properdin**

(A) Idealised images of properdin and properdin-C3bBb convertase complexes generated by combining the averages and the dimensions of experimental single molecule images.

(B) Cartoon representing potential models for the arrangement of subunits at the vertex of properdin oligomers (see Discussion). Alternating oligomers have been coloured differently. The TSR domains are numbered from 0 to 6.

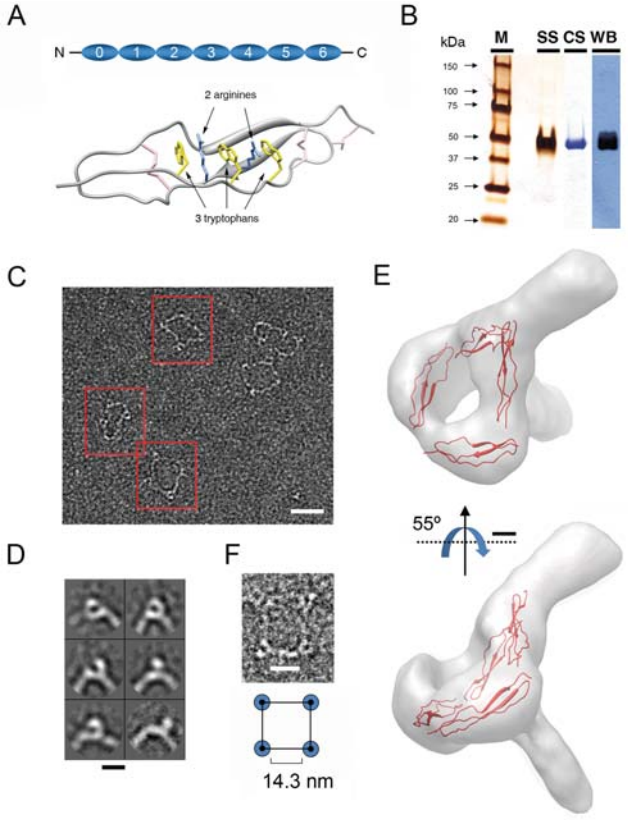
A
N
0
1
2
3
4
5
6
C
2 arginines
3 tryptophans
B
kDa
M
SS
CS
WB
150
100
75
50
37
25
20
C
D
F
14.3 nm
E
55°

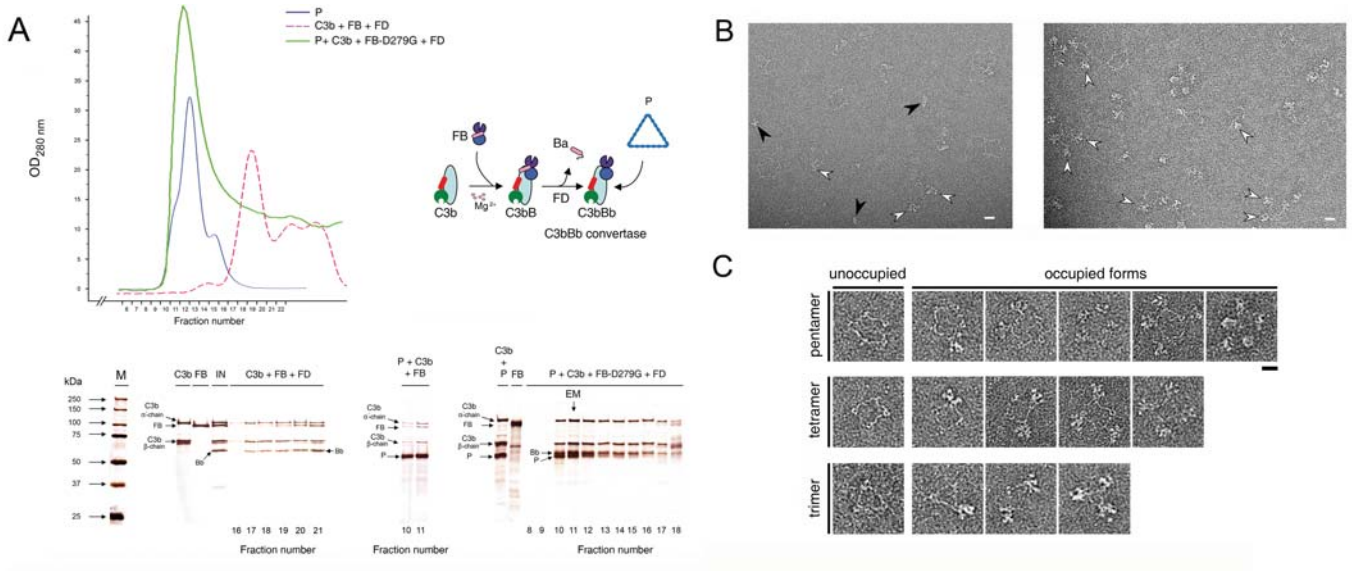
A
P
C3b + FB + FD
P+ C3b + FB-D279G + FD
OD280 nm
Fraction number
FB
Ba
P
C3b
C3bB
FD
C3bBb
C3bBb convertase
kDa
M
C3b FB
IN
C3b + FB + FD
P + C3b + FB
C3b + P FB
P + C3b + FB-D279G + FD
EM
Fraction number
Fraction number
Fraction number
B
C
unoccupied
occupied forms
pentamer
tetramer
trimer

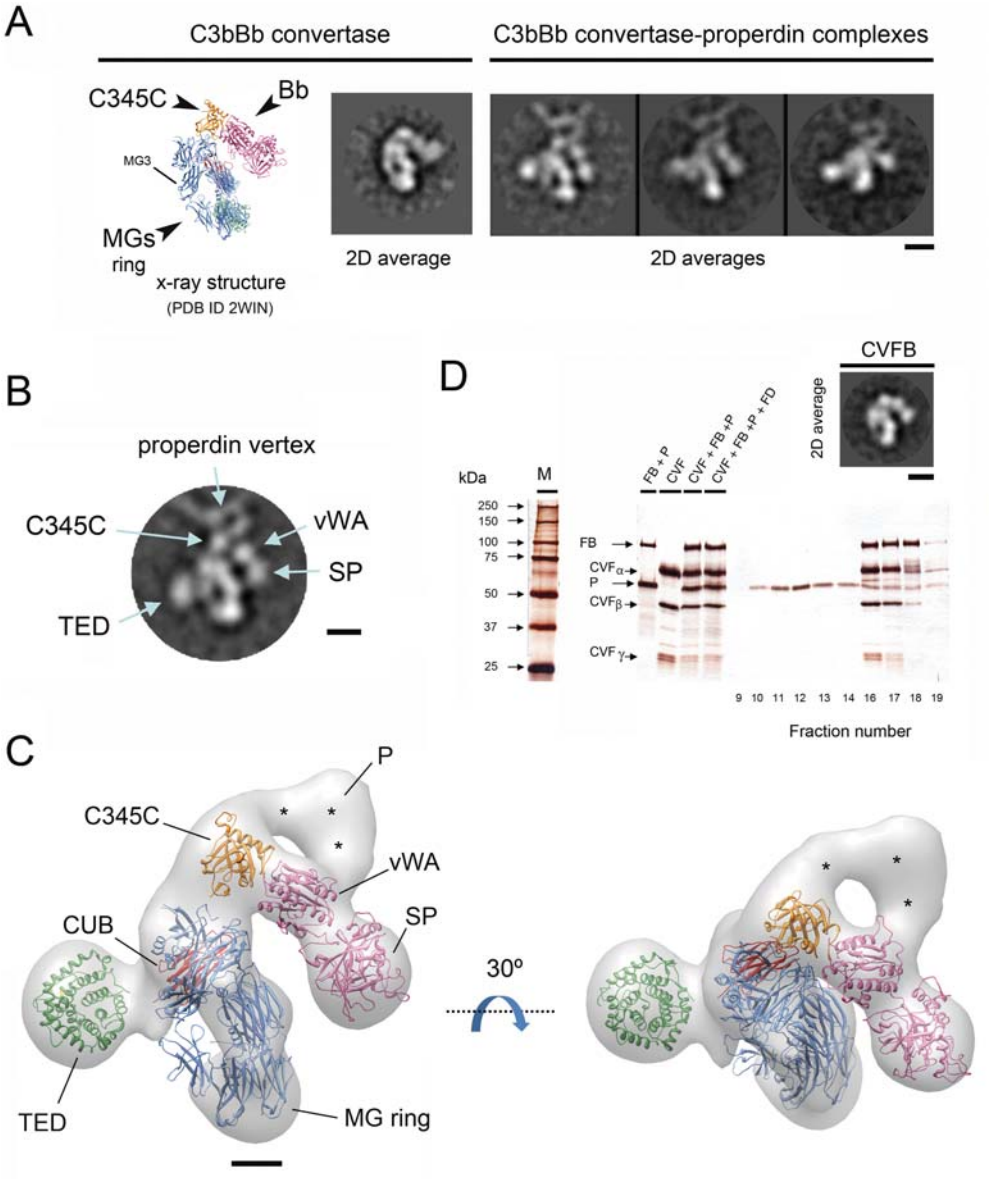
A
C3bBb convertase
C3bBb convertase-properdin complexes
C345C
Bb
MG3
MGs ring
x-ray structure
(PDB ID 2WIN)
2D average
2D averages
B
properdin vertex
C345C
vWA
SP
TED
D
CVFB
2D average
kDa
M
FB + P
CVF
CVF + FB + P
CVF + FB + P + FD
250
150
100
75
50
37
25
FB
CVFα
P
CVFβ
CVFγ
9 10 11 12 13 14 16 17 18 19
Fraction number
C
P
C345C
vWA
SP
CUB
TED
MG ring
30º

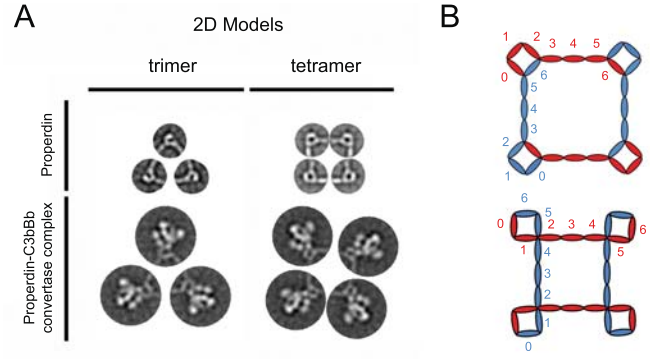
A
2D Models
trimer
tetramer
Properdin
Properdin-C3bBb convertase complex
B

SUPPORTING INFORMATION FOR

Structural basis for the Complement Alternative Pathway C3 convertase stabilization by Properdin

Martin Alcorlo, Agustín Tortajada, Santiago Rodríguez de Córdoba and Oscar Llorca

Supporting Materials and Methods

Purification of C3b, FB and properdin. C3b was produced from C3 purified from plasma as described previously (2). C3 was processed to C3b by adding FB and FD (Calbiochem) in 20 mM Tris, 150 mM NaCl, and 2 mM $MgCl_2$, followed by incubation for 1 h at 37 °C. The product was loaded into a MonoQ column (GE Healthcare) equilibrated with 20 mM Tris (pH 8.6), and the bound protein was eluted using a gradient to 350 mM NaCl. Fractions containing C3b were pooled and dialyzed against 20 mM Tris-HCl (pH 7.6), 150 mM NaCl, and 0.02% (vol/vol) Tween-20. Recombinant FB and FB-D279G were purified from the supernatant of CHO cells as described previously (3). Properdin from human plasma was purified by immunoaffinity chromatography. Briefly, 2 liters of filtered plasma were loaded into an immunoaffinity column coupled to a mouse monoclonal anti-human properdin antibody (mAB 246.111; in house). Bound protein was eluted with 100mM Glycine, pH 2.0 over 2M Tris buffer pH 8.0 to neutralize the elution solution. Fractions containing properdin were pooled and dialyzed against 20 mM $NaPO_4$ (pH 6.4) and 40 mM NaCl, and they were then loaded into a cation exchange MonoS column (GE Healthcare) equilibrated with the same buffer. The bound protein was eluted using a 20 to 500 mM NaCl gradient. Fractions containing properdin were pooled and dialyzed against 20 mM Tris-HCl (pH 7.4), 50 mM NaCl, 50% (vol/vol) glycerol and stored at -80ºC.

Generation and purification of properdin-C3bBb convertase complexes. C3b (5 μg), FB (10 μg, FB or FB-D279G) and properdin (P, 1 μg) were incubated for 35 min at room temperature in 20 mM Hepes (pH 7.5), 75 mM NaCl and 5 mM $MgCl_2$ at a final molar ratio P:C3b:FB 0.7:1:4. Subsequently, 100 ng of FD (Calbiochem) were added and the mixture was injected in a Superdex 200 column (GE Healthcare). Fractions were analysed using 10% SDS/PAGE. The indicated fraction containing the PC3bBb complex was selected for observation using EM.

Western blot analysis. 0.1 μg of properdin was subjected to SDS-PAGE using pre-cast 4-15% polyacrylamide gels (Bio-Rad), and the sample was transferred using a Mini Trans-Blot apparatus (Bio-Rad) at 200 mA and 4°C for 2 hours. Immobilon-P membranes (Millipore) were probed with 1:3000-diluted anti-properdin polyclonal antibodies (in house) for 70 min. Membranes were washed twice and incubated with 1:5000-diluted anti-mouse horseradish peroxidase-conjugated antibodies (DAKO) for 70 min. The immune complexes were detected by ECL detection reagents (Amersham).

Electron Microscopy and Image processing. All preparations were subjected to a final purification step using size-exclusion Superdex 200 chromatography (GE Healthcare) in 20 mM Hepes (pH 7.5), 75 mM NaCl and 5 mM $MgCl_2$ before the preparation of EM grids. A few microliters of freshly purified complexes from a selected fraction were adsorbed onto glow-discharged carbon-coated grids and negatively stained with 2% (mass/vol) uranyl formate. Micrographs were recorded using a JEOL 1230 transmission electron microscope (operated at 100 kV) and a 4 k x 4 k TVIPS CMOS detector using a low-dose protocol under control of the EM-TOOLS software (TVIPS). Images were collected at a final magnification of 54926x. The

contrast transfer function (CTF) for each micrograph was estimated using CTFFIND3 (4) and correction was performed using BSOFT (5). 6425 images for properdin vertexes and 19805 images for C3bBb convertases bound to a propedin vertex were manually selected using EMAN (6). Images were classified and averaged using maximum-likelihood multi-reference methods (7) as implemented in XMIPP (8). *Ab initio* templates for angular refinement were obtained using (i) the command *e2initial model* in EMAN2 (6) and (ii) the random conical tilt (RCT) method (9). For the RTC approach, untilted (0°) and tilted (50°) micrographs were sequentially taken from a particular area in the grid and 3000 pairs of manually extracted particles were used for the RCT reconstruction, performed using XMIPP (8). Additionally, micrographs were recorded at 40° tilting to increase the number of views obtained for properdin vertexes and properdin-C3bBb convertase complexes, and the images extracted were added to the dataset collected without tilting. For processing of the properdin-C3bBb convertase complex the data was split in two structurally distinct populations containing 12324 and 6176 particles respectively, based on 2D classification and the correlation of the images with different starting templates obtained using RCT. 3D reconstructions were obtained using angular refinement using EMAN (6). The resolution of each structure was estimated using Fourier shell correlation and a cut-off of 0.5, and found to correspond to 29.3 Å and 33.0 Å resolution for the major and minor conformation of the properdin-C3bBb complex respectively. Maps and structures were visualized using UCSF Chimera (10). The atomic structure of the C3bBb convertase (PDB ID 2WIN) (11) was fitted within the EM density using the tool *fit in map* implemented in UCSF Chimera (10). Handedness of the reconstructions was defined by the fitting of the MG ring from the crystal structures. Overall, we found a strong agreement between the atomic structures and the EM model, with high cross-correlations for the comparisons between

the crystal and EM structures of the MG ring (cross-correlation, 0.80), the C345C-Bb cassette (cross-correlation, 0.88) and the TED domain (cross-correlation, 0.98).

Cofactor activity in the presence of MCP and FI

Fluid-phase cofactor activity of MCP was determined by C3b proteolysis in a C3bBb convertase formation assay. Purified proteins (C3b, 0.8 μg; FB, 1 μg; FD, 50 ng), were incubated for 5 minutes at 37 °C in the absence or presence of properdin (0.9 and 1.8 μg) in 10 mM Hepes (pH 7.4), 150 mM NaCl and 0.85 mM $MgCl_2$. Next, MCP (0.2 μg) and FI (50 ng) were added and the mixture was incubated for another 15 minutes. Reactions were stopped by adding SDS sample buffer. Samples were analysed by 10% SDS-PAGE under reducing conditions and Coomassie stained. Gels were scanned using a GS-800 calibrated densitometer (BioRad) and the MultiGauge software package (FUJIFILM). To determine the cofactor activity of MCP the amount of remaining C3b after each experiment was estimated as the ratio between α´chain/β chain of C3b. Samples without MCP and FI were used as controls of 100% of intact C3b.

Supporting References

1. Sun Z, Reid KB, & Perkins SJ (2004) The dimeric and trimeric solution structures of the multidomain complement protein properdin by X-ray scattering, analytical ultracentrifugation and constrained modelling. (Translated from eng) *J Mol Biol* 343(5):1327-1343 (in eng).
2. Martinez-Barricarte R*, et al.* (2010) Human C3 mutation reveals a mechanism of dense deposit disease pathogenesis and provides insights into complement activation and regulation. (Translated from eng) *J Clin Invest* 120(10):3702-3712 (in eng).
3. Goicoechea de Jorge E*, et al.* (2007) Gain-of-function mutations in complement factor B are associated with atypical hemolytic uremic syndrome. (Translated from eng) *Proc Natl Acad Sci U S A* 104(1):240-245 (in eng).
4. Mindell JA & Grigorieff N (2003) Accurate determination of local defocus and specimen tilt in electron microscopy. (Translated from eng) *J Struct Biol* 142(3):334-347 (in eng).

5. Heymann JB & Belnap DM (2007) Bsoft: image processing and molecular modeling for electron microscopy. (Translated from eng) *J Struct Biol* 157(1):3-18 (in eng).

6. Tang G*, et al.* (2007) EMAN2: an extensible image processing suite for electron microscopy. (Translated from eng) *J Struct Biol* 157(1):38-46 (in eng).

7. Scheres SH (2010) Classification of structural heterogeneity by maximum-likelihood methods. (Translated from eng) *Methods Enzymol* 482:295-320 (in eng).

8. Sorzano CO*, et al.* (2004) XMIPP: a new generation of an open-source image processing package for electron microscopy. (Translated from eng) *J Struct Biol* 148(2):194-204 (in eng).

9. Radermacher M (1988) Three-dimensional reconstruction of single particles from random and nonrandom tilt series. (Translated from eng) *J Electron Microsc Tech* 9(4):359-394 (in eng).

10. Goddard TD, Huang CC, & Ferrin TE (2007) Visualizing density maps with UCSF Chimera. (Translated from eng) *J Struct Biol* 157(1):281-287 (in eng).

11. Rooijakkers SH*, et al.* (2009) Structural and functional implications of the alternative complement pathway C3 convertase stabilized by a staphylococcal inhibitor. (Translated from eng) *Nat Immunol* 10(7):721-727 (in eng).

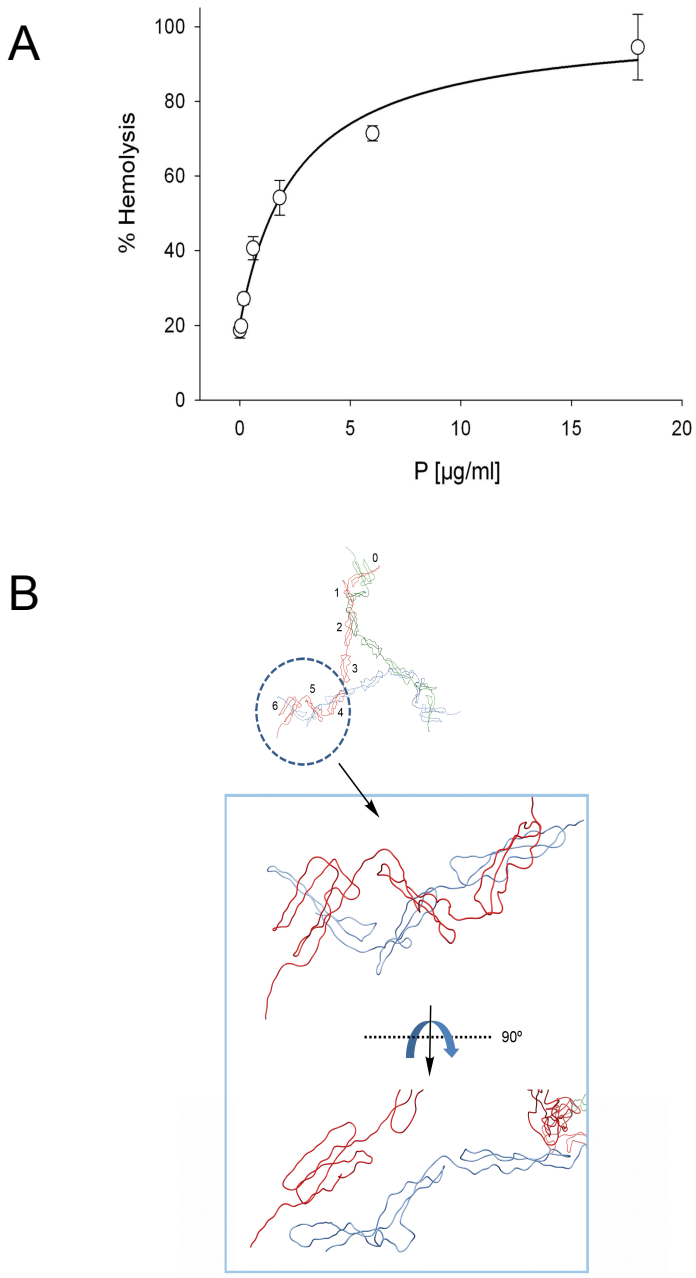

Figure S1. Functional activity and structure of properdin

(A) To assess the functional activity of purified properdin, a hemolytic assay was performed using rabbit erythrocytes. Erythrocytes were incubated with properdin-deficient serum (ΔP) in AP buffer and supplemented with increasing amounts of purified P. Hemolysis observed is shown as percentage of the hemolysis using NHS.

Hemolytic assays were performed to assess the functional activity of our purified properdin. Briefly, normal human serum (NHS) was properdin-depleted by flowing over immovilized anti-properdin (in house). One volume of rabbit erythrocites ($4x10^8$ cells/ml) was diluted in AP buffer (2,5 mM barbital; 1,5 mM sodium barbital, 144 mM NaCl; pH 7,4) with 7 mM $MgCl_2$ and 10 mM EGTA and mixed with one volume of NHSΔP, supplemented with increasing amounts of purified properdin (0.06, 0.18, 0.6, 1.8, 60, 180 μg/ml), and incubated during 15 minutes at 37°C. The reaction was stopped by adding 1 ml of AP buffer containing 20 mM EDTA. After centrifugation, supernatants were red at 414 nm. Lysis mediated by NHS was taken as 100% lysis and NHS diluted in AP plus 20 mM EDTA was used as blank for spontaneous lysis.

(B) Trimer model for properdin proposed by Sun Z, *et al* 2004 (PDB ID 1W0S). The three different chains are shown in red, blue and green. In the inset, an amplified view of the indicated vertex is shown.

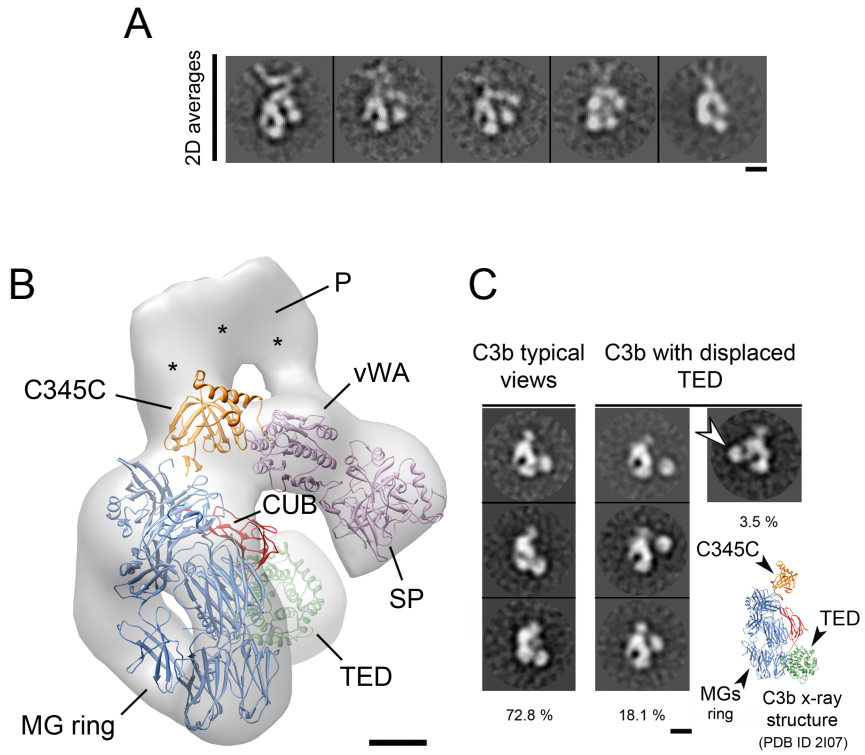

Figure S2. Positioning of the TED domain in the properdin-C3bBb convertase complex

(A) Representative 2D averages of the minor conformation of the properdin-C3bBb convertase complex. These show that the TED domain is not in the proximities of the MG3 domain, but in the location found in the crystal structure of C3b. Scale bar corresponds to 5 nm.

(B) One view of the structure of the minor conformation of the properdin-C3bBb convertase complex at 33.0 Å resolution. Scale bar corresponds to 2 nm.

(C) Processing and classification of images of C3b revealed that most molecules show the TED domain in the classical conformation, whereas a small percentage of molecules display the TED domain in alternative conformations. An arrow points to the TED domain placed close to the MG3 domain, found in 3.5 % of the images analysed. A view from the crystal structure of C3b (PDB ID 2I07) is shown to help comparison with the EM images. Each domain has been coloured differently and labelled. Scale bar corresponds to 5 nm.

(D) C3bBb convertase was formed by incubating C3b, FB and FD in the absence or presence of properdin (P) (0.9 μg; grey or 1.8 μg; black), and incubated with MCP and FI. SDS-PAGE shows the result of this reaction after incubating for 15 min.

(E) The amount of C3b remaining after incubation was estimated by quantifying the ratio between α´chain/β chain of C3b. Error bars indicate the mean ± SD of two independent experiments.